

Florida Institute of Technology

## Scholarship Repository @ Florida Tech

---

Theses and Dissertations

---

8-2020

### Performance Analysis of V2V and V2I Communications Using Empirical Path Loss Models Indicators and Embedded IoT Devices

Ibrahim Lateef Oraibi Al Kinoon

Follow this and additional works at: <https://repository.fit.edu/etd>



Part of the [Computer Engineering Commons](#)

---

Performance Analysis of V2V and V2I Communications Using Empirical Path  
Loss Models Indicators and Embedded IoT Devices

by

Ibrahim Lateef Oraibi Al Kinoon

A dissertation submitted to the College of Engineering and Science of  
Florida Institute of Technology  
in partial fulfillment of the requirements  
for the degree of

Doctor of Philosophy

in

Computer Engineering

Melbourne, Florida

August, 2020

© Copyright 2020 Ibrahim Lateef Oraibi Al Kinoon  
All Rights Reserved

The author grants permission to make single copies \_\_\_\_\_

We the undersigned committee hereby approve the attached dissertation,  
“Performance analysis of V2V and V2I Communications Using Empirical Path  
Loss Models Indicators and Embedded IoT Devices.”

by  
Ibrahim Lateef Oraibi Al Kinoon

---

Carlos Enrique Otero, Ph.D.  
Associate Professor  
Computer Engineering  
Major Advisor

---

Ersoy Subasi, Ph.D.  
Assistant Professor  
Systems Engineering

---

Susan Earles, Ph.D.  
Associate Professor  
Electrical Engineering

---

Ivica Kostanic, Ph.D.  
Associate Professor  
Electrical and Computer Engineering

---

Philip Bernhard, Ph.D.  
Associate Professor and Department Head  
Computer Engineering and Sciences

# Abstract

Title: Performance analysis of V2V and V2I Communications Using Empirical Path Loss Models Indicators and Embedded IoT Devices

Author: Ibrahim Lateef Oraibi Al Kinoon

Advisor: Carlos E. Otero, Ph. D.

Vehicle management technologies deals with the management of critical vehicle information, including location, idle time, speed, and mileage. Such information can always be transferred through a direct vehicle-to-vehicle communication among cars. However, the limitation of this type of design is that it is based on the assumption that vehicles are always served by cellular bases, which is not always the case. For the effective implementation of the Internet-of-Things (IoT) technology in this sector, it is critical to design vehicles with systems that enable them to transmit essential information in the absence of base stations. IoT technologies can then be used to develop mesh communication between devices to replace the need for cellular service. This project proposes models that can be used to design self-reporting systems for vehicles to enhance self-management. The study also compares

the proposed models with theoretical models, which show deviations of between 6% and 23%. The overall efficiency of vehicle-to-vehicle (V2V), vehicle-to/from-infrastructure (V2I) or vehicle-to/from-environments can only be attained if there is a reliable exchange of information between the communicating vehicles. Reliable exchange of information also enhances the overall efficiency with which self-driving cars and autonomous vehicle technologies can be implemented. Such systems require not only a variety of IoT systems, but also a series of sensors and nodes for effective transfer of information, the processing of information, and quick decision-making. However, the heterogeneous environments and overall ecosystems pose reliability changes on the information transmitted to be processed by the ecosystem in order to guarantee the safety and functional operation of the ecosystem. This study examines the reliability of the communication model that can support the operation of self-driving cars ecosystem. It also shows semi-empirical energy per bit to noise spectral density, empirical radio propagation models and parameters for driving and transportation environment. These values and models, which are obtained from a combination of the experimental approach and analytical approach of additive white Gaussian noise channel are used to ensure a reliable communication of wireless sensor nodes deployed in the environments for V2V, V2I, and V2X services. Additionally, the values and models are validated in theoretical and semi-analytical simulation scenarios. The results indicate that both techniques are nearly identical. The semi-empirical approach, the proposed models, and values can be

used for efficient planning and future deployments of autonomous vehicles and self-driving cars.

# Table of Contents

List of Figures .....	viii
List of Tables.....	ix
Acknowledgement.....	x
Dedication .....	xii
Chapter 1 Introduction .....	1
1.1 Motivation .....	1
1.2 Dissertation Outline .....	2
1.3. Machine Type Communication (MTC) .....	3
1.3.1 Vehicle to Vehicle Communications .....	4
1.4. Low Power Wide Area Network (LPWAN).....	6
1.4.1. LPWAN Using Cellular Protocols.....	7
1.4.1.1 Narrow Band – Internet of Things (NB-IoT).....	7
1.4.1.2 LTE–M.....	12
1.4.2. LPWAN Using Non-Cellular Protocols.....	13
1.4.2.1. Sigfox .....	14
1.4.2.2. LoRa.....	14
1.4.2.3. Symphony .....	15
1.5. Path Loss .....	15
1.6. Propagation Models .....	16
1.6.1. Free Space Model.....	17
1.6.2. Tow-Ray Model .....	20
1.6.3. Log Distance Path Loss Model .....	22
Chapter 2 Empirical Path Loss Model for Vehicle-to-Vehicle.....	25
2.1. Abstract .....	25



2.2. Introduction .....	26
2.3. Literature Review .....	29
2.4. Methodology .....	31
2.4.1. Experimental Campaign and Measured Values .....	31
2.5. Preliminary Results and Discussion.....	35
2.5.1. Empirical Models .....	35
Chapter 3 Reliability Analysis of V2V Communications Link .....	40
3.1. Abstract .....	40
3.2. Introduction .....	41
3.3. Literature Review .....	42
3.4. Experimental Campaign.....	45
3.5. Analysis and Results .....	48
References .....	57

# List of Figures

Figure 1.1 — LTE Communication. ....	2
Figure 1.2 — Three Models of Operation.....	11
Figure 1.3 — A Summary of Technologies Driving the IoT Market. ....	13
Figure 2.1 — Pictorial Diagram for In-Car Measurement. ....	32
Figure 2.2 — Path Loss Model Plot for Sedan-to-Sedan, A Node on the Car Floor .....	37
Figure 2.3 — Path Loss Model Plot for Sedan-to-Sedan, A Node at Seat Height.....	37
Figure 2.4 — Path Loss Model Plot for Sedan-to-Sedan, A Node on the Floor with 18 dBm Node. ....	38
Figure 2.5 — Path Loss Model Plot for Sedan-to-Sedan, A Node at Seat Height with 18 dBm Node. ....	38
Figure 3.1 — Plot for SNR Against Distance. ....	53
Figure 3.2 — Spectral Efficiency vs. Energy Per Bit to Noise Spectral with Higher Values of $E_b/N_0$ (Db).....	54
Figure 3.3 — Plot for Spectral Efficiency vs. Energy per Bit to Noise Spectral V2V Communications. ....	55
Figure 3.4 — Plot of Theoretical and Simulated BER vs. Energy Per Bit to Noise Spectral.....	55

## List of Tables

Table 2.1 — Average Path Loss at 2.74 m Interval Using 3 dBm Node .....	33
Table 2.2 — Average Path Loss at 6.52 m Interval Using 18 dBm Node .....	33
Table 2.3 — Summary of Proposed Models, Parameters, and Percentage Deviation .....	34
Table 2.4 — Statistics for Comparison Between Theoretical Models and Proposed T1 Model .....	39
Table 3.1 — Average Path Loss at 2.74 m Interval Using 3 dBm Node .....	47
Table 3.2 — Average Path Loss at 6.52 m Interval Using 18 dBm Node .....	47
Table 3.3 — Summary for Comparison Between Theoretical Models and Proposed T1 Model .....	48

# Acknowledgement

All Thanks and praise is due to Allah the Almighty. I thank Him for His countless bounties and generous blessings upon us. I thank Him for Providing me the opportunity and granting me the capability to successfully complete this work.

I would also like to express my deepest appreciation and sincere gratitude to my advisor Dr. Carlos Otero for his motivations, guidance, and his continuous support. The knowledge I gained and the experience I acquired from working with him have made my academic and experimental background better. It is an honor for me to conduct research study under his supervision. Many thanks go to all the professors at Florida Tech who have taught me courses and for their helps in achieving academic excellence.

I am also very grateful to a few people who supported me throughout my research journey. First, I am thankful to my parents for their endless love, support, prayers, and patience during the time I studied abroad. I would like to pass my special thanks to my wife for her love, support, patience, and understanding during this long time of study. My special appreciation goes to my sons and daughters (Noor, Mohammed, Nadia, Ali, Hussein, Mustafa, and Rose) for patience, being source of inspiration and for their moral and financial support. I am privileged to have them as my family. My sincere gratitude goes to my sisters for their support and encouragement.

I also thank my committee members, Dr. Carlos Otero, Dr. Ivica Kostanic, Dr. Susan Earles, Dr. Muzaffar Shaikh and Dr. Ersoy Subasi for their leadership and time. I extend my special thanks and acknowledgement to my friends Dr. Tajudeen Olawale Olasupo and Engineer Hayder Shakir Najm for their help and support. Finally, I thank all the people who help me to achieve my goal and reach this very essential milestone in my life.

## Dedication

*To:*

*My father and mother for their love, prayers, endless support and encouragement*

*My wife for her love, support, encouragement, patience and understanding*

*My sons and daughters for their love, patience and unending supports and inspiration*

*My sisters and friends for their love and supports*

*The soul of the martyr, my dearest sister, Um Abdullah*

# Chapter 1

## Introduction

### 1.1 Motivation

LTE communication can be LTE for mobile communication that means video streaming, broadband, high speed and large file download and LTE for IOTs LTE that includes Machine type communication (MTC) and internet of things. There are two ways of communications for IoT devices, one is the mesh network that each IoT device or sensor connects directly to another without the existence of cellular network (no coverage) and the second type of IoT communications is the cellular communications and in this type of communications there are no direct communications between IoT device and another but they communicate through a cellular network. Mesh network is important when many devices in the same area or cellular coverage is not available, for example, vehicle to vehicle communications without the cellular network coverage and when the devices talk to each other frequently, means continuous communications between the IoT devices or sensors. Cellular IoT network is important when a few devices in the

same area and when the devices need to talk to the cloud and literary need to talk to each other. Fig 1.1 depicted the two main types of communication.

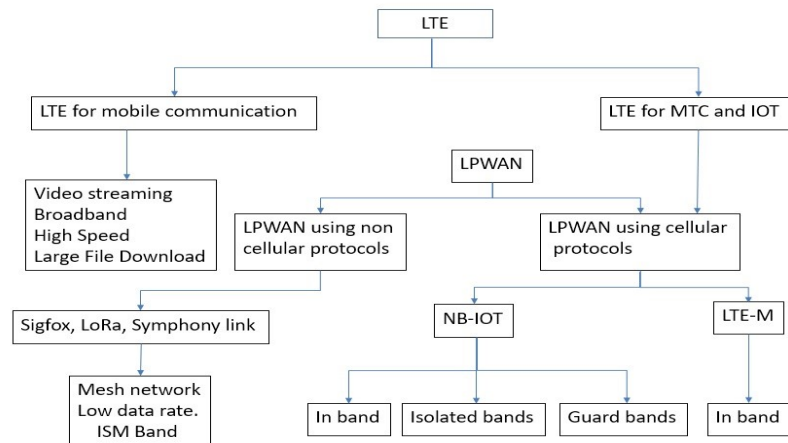


Fig 1.1 LTE Communication

## 1.2 Dissertation Outline

This Dissertation has been organized into three distinct chapters where each chapter contains specific pieces of information that relate to both the preceding and the proceeding chapter. The main contents of the chapters are as follows:

Chapter 1: This chapter introduces the project by analyzing the project's underlying concepts, like LTE communication, machine type communication (MTC), V2V communication, and low power wide area networks (LPWAN).



Chapter 2: This chapter discusses the empirical path loss model for V2V IoT device communication in fleet management systems.

Chapter 3: The main purpose of this chapter is to perform a reliability analysis of V2V and V2I communication link using empirical path loss model indicators and IoT devices.

### 1.3. Machine Type Communication (MTC)

MTC or Machine to machine (M2M) communication, a narrowband system is attractive due to the following reasons: Low cost, especially on the device side. Narrow bandwidth requires less expensive RF components. Also, there is a cost reduction on the baseband side due to the lower data rates, Coverage improvement due to the ability to concentrate transmission power in a narrow bandwidth. Efficient spectrum utilization as smaller bandwidth is needed. For example, LTE-M can be deployed by reframing only one GSM channel, or it can be deployed on a guard band of an existing LTE deployment. An important feature of LTE-M is that it shares the same numerology as LTE. This allows for sharing spectrum between the two systems without causing mutual interference [1].

The study on MTM communications indicated the potential for machine-type communications (MTC) over mobile networks. However, for example, wireless

sensor networks (e.g. ZigBee) in combination with fixed network communications are also a contender for the implementation of such applications. For mobile networks to be competitive for mass machine-type applications, it is important to optimize their support for machine-type communications. The current mobile networks are optimally designed for Human-to-Human communications but are less optimal for MTM, machine-to-human, or human-to-machine applications. It is also important to enable network operators to offer MTC services at a low-cost level, to match the expectations of mass-market machine-type services and applications [2].

### 1.3.1 Vehicle to Vehicle Communications

At present, V2V communication systems are likely to be deployed using spectrum in the 5GHz band—5.9GHz in the U.S. and 5.7GHz in Europe (in fact, allocation of spectrum in this band provided some of the first real impetus behind V2V research). such systems are also expected to operate in vehicle-to-infrastructure (V2I) mode, wherein the communication is between cars and base stations or access points distributed along roadways. The future ITS will also incorporate traditional cellular communications, and potentially even wireless local area networks (WLANs) where available; these communication links will employ spectral bands outside those of V2V/V2I systems, and overall coordination of these multiple systems, including

coordination and the use of Global Positioning System information, is still being researched [3].

Actual models for the V2V channel can and often do include the effects of antennas and possibly parts of antenna processing (indeed, it is often challenging to separate out antenna effects from measurements). Additional processing such as that from filters, diplexers, and other parts of conventional radio transceivers may also be included in measurement-based models unless modelers take explicit steps to deem such effects. Nonetheless, with or without express inclusion of such effects, it has become conventional in wireless communications for terrestrial environments to model the effects of the channel as composed of three generally distinct mechanisms: path loss, shadowing, and small-scale fading. Path loss (or its reciprocal, path gain), accounts for the distance-dependent decay of received signal strength. In free space, this, of course, arises as the power density of a propagating wave diminishes with distance from the source [3]. Prediction of the path loss is a fundamental task in cellular systems deployment. To accomplish this task, engineers rely on propagation modeling that estimates the average signal strength and consequently the path loss that tacitly also includes average additional attenuation due to obstruction [4]. Shadowing (sometimes termed obstruction or blocking) is a large-scale “fading” effect that is attributed to the attenuation caused by large obstacles concerning a wavelength, e.g., terrain or buildings. In V2V settings, this can also include obstacles

such as buses or trucks. At VHF and higher frequencies, where such obstacles are much larger than a wavelength, shadowing effects are distinct from the small-scale effects of multipath fading, although conflating or at least combining shadowing and path loss effects is quite common. Hence, the most widely used model for path loss and shadowing expresses their effects jointly via the “log distance” path loss model [3].

#### 1.4. Low Power Wide Area Network (LPWAN)

LPWAN is a broad term for a variety of technologies used to connect sensors and controllers to the internet without the use of traditional Wi-Fi or cellular. LPWAN was created to describe a portion of the Internet of Things (IoT) and machine-to-machine (M2M) market. Most of these LPWAN solutions use the ISM (Industrial Scientific and Medical) bands better known for use by short-range wireless technologies like ZigBee, Wi-Fi, and 6LoWPAN. However, recent advances have enabled LPWANs to be established using the ISM bands over longer distances, up to 50km in rural areas and 5-10km in urban areas[5]. LPWAN protocols can be divided into LPWAN using cellular protocols and LPWAN using non-cellular protocols.

### 1.4.1. LPWAN Using Cellular Protocols

LPWANs that used non-cellular protocols are working using the ISM bands over longer distances, up to 50km in rural areas and 5-10km in urban areas. Non-cellular enjoys distinct advantages over cellular; they offer lower power, low bandwidth, and low-cost solutions – which is right for a variety of IoT applications. Nevertheless, the scale of cellular LPWA deployments is expected to be much larger than non-cellular LPWANs. But each technology will create their own space within the market as enterprises move ahead in their learning curve.

#### 1.4.1.1 Narrow Band – Internet of Things (NB-IoT)

NB-IoT is the 3GPP radio-access technology designed to meet the connectivity requirements for massive MTC applications. In contrast to other MTC standards, NB-IoT enjoys all the benefits of the licensed spectrum, the feature richness of EPC, and the overall ecosystem spread of 3GPP. At the same time, NB-IoT has been designed to meet the challenging TCO structure of the IoT market, in terms of device and RAN cost, which scales with transferred data volumes. The specification for NB-IoT is part of 3GPP release 13 and it includes many design targets: device cost under USD 5 per module; a coverage area that is seven times greater than existing 3GPP

technologies; device battery life that is longer than 10 years with sustained reachability; and meet a capacity density of 40 devices per household.

As NB-IoT can be deployed in the GSM spectrum, within an LTE carrier, or in an LTE or WCDMA guard band, it provides excellent deployment flexibility related to spectrum allocation, which in turn facilitates migration. Operation in a licensed spectrum ensures that capacity and coverage performance targets can be guaranteed for the lifetime of a device, in contrast to technologies that use unlicensed spectrum, which run the risk of uncontrolled interference emerging even years after deployment, potentially knocking out large populations of MTC devices [6].

The new technology (NB-IoT) will provide improved indoor coverage, support of a massive number of low-throughput devices, low delay sensitivity, ultralow device cost, low device power consumption, and optimized network architecture. The technology can be deployed in-band, utilizing a carrier, or in the unused resource blocks within an LTE carrier's guard-band or stand-alone for deployments in a dedicated spectrum. The NB-IoT is also particularly suitable for the refarming of the Global System for Mobile Communications (GSM) channels [7].

The LPWAN market has existed for about 10 years; it's not a new thing. The current technologies (solutions) supporting this market are fragmented and non-standardized, therefore there are shortcomings like poor reliability, poor security, high operational and maintenance costs. Furthermore, the new overlay network

deployment is complex. NB-IoT overcomes the above defects, with all the advantages like wide-area ubiquitous coverage, fast upgrade of the existing network, low-power consumption guaranteeing 10-year battery life, high coupling, low-cost terminal, plug and play, high reliability and high carrier-class network security, unified business platform management. Initial network investment may be quite substantial and superimposed costs are very little. NB-IoT perfectly matches LPWAN market requirements, enabling operators to enter this new field. NB-IoT enables operators to operate traditional businesses such as Smart Metering, Tracking, by virtue of ultra-low-cost (\$ 5) modules and super connectivity (50K / Cell), also opens up more industry opportunities, for example, Smart City, eHealth. The reasons are simple: Coverage, battery life, and device cost. First, coverage: Existing cellular networks already offer very good area coverage in mature markets. However, many potential “connected objects” are located in vast remote areas, far away from the next cellular base station. If there is coverage, it is often weak which requires the device transmitter to operate at high power, draining the battery. Also, cellular networks are not optimized for applications that occasionally transmit small amounts of data. A battery life of several years combined with an inexpensive device cannot be realized on existing cellular standards, as they do not support the required power saving mechanisms.

To realize this, it is ideal to have about 50K devices per cell; this is possible assuming there is the household density per every sq. m is 1500 with 40 devices in every household. When we compare the inherent capabilities of NB-IoT with other LPWAN technologies like e-MTC, SigFox, and Lora, NB-IoT offers better performance. Furthermore, when we look at all the technologies in terms of network investment, coverage scenario, uplink, and downlink traffic and network reliability we realize that NB-IoT is the most suitable technology. Additionally, from a performance point of view, NB-IoT guarantees 20+dB coverage, ~1000x connections, ~10 years using only 200 kHz bandwidth whereas the other technologies like eMTC, SigFox offers far less in terms of performance.

NB-IoT will offer three deployment scenarios; these are, Guard Band, In-Band and Stand Alone. Standalone deployment is mainly utilized new bandwidth whereas guard band deployment is done using the bandwidth reserved in the guard band of the existing LTE network, In-Band, on the other hand, makes use of the same resource block in the LTE carrier of the existing LTE network [8],[9]as in fig 1.2.



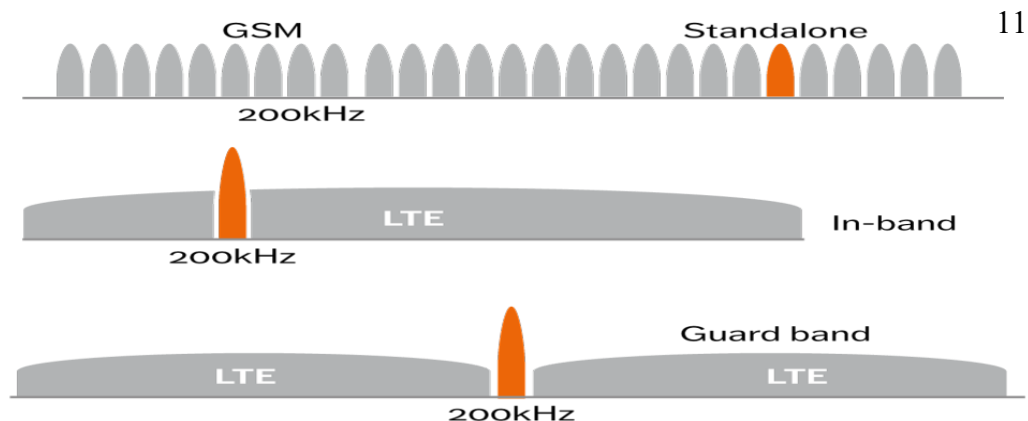


Fig 1.2. Three modes of operation for NB-IoT

It is worth noting that the application of NB-IoT includes and not limited to smart cities, Medical & health, smart home, building automation, smart metering & smart grid, fleet management systems and retail vending.

To enable such small bandwidth allocations, NB-IoT uses tones or subcarriers instead of resource blocks. The subcarrier bandwidth for NB-IoT is 15kHz, compared with a resource block, which has an effective bandwidth of 180kHz. Each device is scheduled on one or more subcarriers in the uplink, and devices can be packed even closer together by decreasing the subcarrier spacing to 3.75kHz. Doing so, however, results in differing numerology for LTE and NB-IoT, and some resources will need to be allocated to avoid interference between the 3.75kHz and 15kHz subcarriers instead of utilizing them for traffic, which may lead to performance losses [6].

### 1.4.1.2 LTE-M

LTE-M is the abbreviation for LTE Cat-M1 or Long-Term Evolution (4G), category M1. This technology is for the Internet of Things devices to connect directly to a 4G network, without a gateway and on batteries [10].

LTE-M—an abbreviated version of LTE-MTC (or "machine-type communications")—is part of 3GPP's release 12 and 13, finalized in 2016. It is also referred to as LTE-MTC or LTE Cat M1.

In the simplest terms, LTE-M is a stripped-down version of LTE. It uses the same spectrum and base stations, works everywhere that LTE works, and enables true TCP/IP data sessions. The major difference between LTE and LTE-M is power efficiency—LTE-M enables battery-powered devices to send and receive data online via a Verizon or AT&T connection. An iPhone battery lasts a day, but a cell modem-connected water meter battery could last 10 years—which is a profound change to the cellular Internet of Things. LTE-M has a slightly higher data rate than NB-IoT and EC-GSM-IoT but can transmit fairly large chunks of data. Potential applications include tracking objects, energy management, and utility metering; this technology could also be used in city infrastructure and wearable devices[11] new.

### 1.4.2. LPWAN Using Non-Cellular Protocols

Some applications that require global coverage and/or mobility will use cellular technologies, but the majority of IoT devices will use non-cellular technologies' sharing frequencies in unlicensed bands to communicate with each other and with IoT applications in the cloud.

New technologies are being developed for Low Power WAN (LP-WAN), including SIGFOX, LoRa, Weightless, and Ingenu. In the Wide Area Networks (WAN), there are well-known cellular technologies (2G,3G,4G), with new feature enhancements like eMTC and NB-IoT as in fig 1.3. This section gives a short introduction to the emerging wireless technologies for the IoT market.



Figure 1.3. Summary of Technologies driving IoT Market

Low Power WAN (LP WAN) devices are everywhere and networks to support these devices are being deployed all over the world. They operate in the unlicensed ISM band, using new technologies such as Long Range (LoRa), SIGFOX, Weightless and Ingenu [12].

#### 1.4.2.1. Sigfox

The SIGFOX technology is aimed at low-cost machine-to-machine application areas, where wide area coverage is required. SIGFOX uses the 915GHz ISM band in the US, with its patented Ultra Narrow Band (UNB) technology. UNB enables very low transmitter power levels to be used while still being able to maintain a robust data connection. SIGFOX messaging has a payload size of just 12 bytes, a maximum throughput of 100bps and uses a narrowband (100Hz) channel [12].

#### 1.4.2.2. LoRa

Lora another protocol of LPWAN that uses wider bandwidth and it is not an open standard and it is distributed as a sim chip, the security is very good and uses all the very good basic authentications and a good chance of deployment in Europe and it is not available in the US.

### 1.4.2.3. Symphony

Symphony Link is a wireless solution for enterprise and industrial customers who need to securely connect their IoT devices to the cloud and it is the only LPWA System with Repeaters, 100% Acknowledgment, quality of services and Firmware over the air. Wi-Fi [33] and ZigBee ranges are too limiting, cellular is too expensive and power-hungry, and most LPWAN systems do not have the features necessary for your application. Symphony Link is specifically designed for low power, wide-area network (LPWAN) applications that are easily scalable and perform with best-of-class reliability. One of the most important features of this LPWA system is the real-time power and data rate control [13].

## 1.5. Path Loss

In wireless communication system signals travel between transmit antenna and receive antenna through a channel. The channel is a fundamental part of wireless system deployment and has an essential role in system performance. In general, when the signal travels its level decreases with the increasing distance between a source (base station, relay station or mobile station) and destination (mobile station, relay station or base station). The degradation in the transmitted signal power as it propagates in space is referred to as path loss. Prediction of the path loss is a

fundamental task in cellular systems deployment. One of the requirements of designing base stations in cellular networks is to have a basic understanding of coverage areas of each base station. Finding the coverage area of each base station through measurement is impractical since it can be a very expensive and time-consuming process. Instead, engineers rely on propagation modeling that estimates the average signal strength and consequently the path loss at any particular distance from the base station. While an overestimation of path loss can result in extensive coverage overlaps, an underestimation can lead to coverage holes. Path loss is a function of various factors such as free space losses, diffraction, reflection, refraction, transmission frequency, terrain, and many others. Numerous propagation models have been derived and studied, however; there is no single model can be applied for all the environments. As a result, the Quality of Service (QoS) of the whole cellular network depends on the selection of most suitable of the radio propagation model [14].

## 1.6. Propagation Models

One of the fundamental parameters of designing cellular communication systems is the received signal level. To predict the average received signal level, propagation models are used. In this regard, propagation modeling becomes a very significant

tool to study. Signal attenuation (or path loss) prediction and received signal level prediction are two faces of the same coin. In other words, if one can predict the median path loss then the median received signal level is implicitly known. The path loss is simply the difference, expressed in decibels, between the transmitted signal and the received signal power. Path loss includes all possible losses which result from the free space propagation and other different propagation mechanisms. In general, it is also a function of other parameters like antenna heights, carrier frequency, distance, environment type (urban, suburban, or rural) ... etc. Models that are used for predicting the path loss in macro-cells, which are usually encountered in cellular networks, are called macroscopic propagation models. There are many of them and they have different levels of accuracy and complexity. In general, there is a tradeoff between model simplicity and its accuracy. Macroscopic propagation models can be classified into three main categories: basic propagation models, statistical propagation models and deterministic models [14]. Examples of the propagation models that used in comparison with the developed path loss models are:

### 1.6.1. Free Space Model

The major assumption in free space propagation is that there is a clear line of sight (LOS) between transmitter and receiver, meaning that no obstructions exist. In other

words, waves travel without reflection, diffraction, scattering, or any other mechanisms. This model is used to predict the received signal power at a particular distance. Satellite communication systems and microwave links are a typical example of such kind of models. The received signal power  $P_r$  at distance  $d$  from the transmit antenna can be given as: [14]

$$P_r = P_T \frac{G_{TX}G_{RX}}{(4\pi d\lambda)^2} \quad (1.1)$$

Where

$G_{TX}$  - Received power at distance  $d$  from the transmitter

$P_T$  - Transmit power

$G_{RX}$  - Gain of transmitting antenna - Gain of receiving antenna

$\lambda$  - Wavelength

$d$  - Distance between the transmitter and receiver.

The propagation loss is usually expressed in decibels (dB) and it is given by

$$L[\text{dB}] = 10 \log\left(\frac{P_T}{P_r}\right) \quad (1.2)$$

Therefore



$$L[dB] = 10 \log \left[ \frac{(4\pi d/\lambda)^2}{C_{TX} C_{RX}} \right] \quad (1.3)$$

Since

$$\lambda = \frac{c}{f} \quad (1.4)$$

Where

C - Light velocity in space [ $3 \cdot 10^8$  m/sec]

f - Operating frequency

Substituting (1.4) in (1.3) one gets:

$$\left[ L[dB] = 10 \log \left[ \frac{(4\pi f d)^2}{G_{TX} G_{RX}} \right] \right]$$

$$L(dB) = -g_{TX} - g_{RX} + 20 \log(f) + 20 \log(d) + 20 \log(4\pi/C) \quad (1.5)$$

Free space path loss, which represents the attenuation of the signal power, is defined as the difference in dB between the effective transmitted power and received power. When antenna gains are excluded, then the free space path loss ( $PL_{fs}$ ) can be given as

$$PL_{fs}[dB] = 32.44 + 20\log(f) + 20\log(d) \quad (1.6)$$

where now the frequency  $f$  is in units of MHz and distance  $d$  in units of Km.

If  $d$  is expressed in miles, then Eq. (4.6) can be written as:

$$PL_{fs}[dB] = 36.5 + 20\log(f) + 20\log(d) \quad (1.7)$$

Equations (1.6) and (1.7) are called Friis equations [6]. It is noteworthy to observe that free space increases 20 decibels per decade of either frequency or distance. In other words, free space path loss increases by 6 dB for each doubling in either frequency or distance [14].

### 1.6.2. Two-Ray Model

Unlike the free space propagation model where there is only a direct path between the transmitter and the receiver, here, as the name says, the received signal is a sum of two components results from two different paths. The first path is the direct or LOS path and the second one is the ground reflected path [14].

The formula of path loss for this model is expressed as:

$$PL = 40\log(d) - 20\log(h_b) - 20\log(h_m) \quad (1.8)$$

where,

$d$  : Distance between transmitter and receiver in meters.

$h_b$ : Height of the transmitter antenna in meters.

$h_m$  : Height of the receiver (mobile) antenna in meters.

Remarkably, the path loss here increases by 40 dB/dec as a function of distance or 12 dB by doubling the distance. It is also notable that the path loss depends on antenna heights of transmitter and receiver. The other observation that can be made here is that PL is frequency independent. One of the drawbacks of the two-ray model is that it underestimates the path loss because of two major reasons. In practice, the loss is almost always frequency dependent. Second, in this model, the ground was assumed flat and smooth which is in reality not the case. The roughness of the terrain can lead to scattering which in turn affects the total value of the signal power and consequently the path loss [14].

### 1.6.3. Log Distance Path Loss Model

In general, the path loss at any particular location can be seen as consisting of three major components: loss due to distance between transmitter and receiver, log-normal shadowing (large scale fading or slow fading) and small scale fading (fast fading). In the first-order approximation, the predicted path loss in [dB] at any given distance  $d$  from the transmitter with respect to a reference distance  $d_0$  may be described as long-distance path loss model and given by [14].

$$PL(d) = PL_0 + m \log \left( \frac{d}{d_0} \right) \quad (1.9)$$

Where

$d_0$  - Reference distance (usually 1km or 1 mile in macro-cells and 100 m in microcells)

$PL_0$  - Path loss at the reference distance (intercept)

$d$  - Distance between transmitter and receiver

$m$  - Slope in [dB/decade] which can be given as:

$$m = 10n \quad (1.10)$$

where  $n$  is the path loss exponent. The values of  $PL_0$  and  $n$  depend on the environment and they are usually determined through statistical analysis of path loss data measurements. Equation (1.9) expressed the average large-scale path loss at a given distance ( $d$ ). Graphically,  $PL$  is a linear function of ( $d$ ) in the logarithmic domain.

When the actual path loss data are plotted, they show variations about the median path loss given by the model in (1.9). The variations are introduced by log-normal shadowing which occurs since different locations at the same distance from the transmitter might have a different environment and therefore the path loss value is different. The  $PL(d)$  can be considered as a random variable that is normally distributed in log-domain [14] and it is given as:

$$PL(d) = PL_0 + m \log \left( \frac{d}{d_0} \right) + X\sigma \quad (1.11)$$

where  $X\sigma$  is a log-normally distributed random variable that describes the shadowing effects and it can be expressed as:

$$X_\sigma \sim N(0, \sigma)$$

The operator expressed by  $(\sim)$  means that  $X_\sigma$  is a zero-mean Gaussian distributed random variable with a standard deviation of  $\sigma$ . As the model becomes more accurate, the standard deviation  $\sigma$  of the unexplained portion ( $X_\sigma$ ) of path loss becomes smaller. Similar to the path loss exponent  $n$ ,  $\sigma$  is environmentally dependent [14].

## Chapter 2

### Empirical Path Loss Model for Vehicle-to-Vehicle.

#### 2.1. Abstract

Vehicle fleet management systems can monitor and provide accurate vehicle management information, such as location, idle time, speed, and mileage (among others). This information can be transmitted using direct communication between cars and base stations. However, this concept assumes that vehicles are always served by a cellular base station, which is not always the case. In order to fulfill the vision of Internet-of-Things (IoT), where “things” self-manage themselves, there needs to be a mechanism for vehicles to transmit important information in cases where base stations are not available. In these cases, IoT sensing devices can be used to establish device-to-device mesh communication networks between vehicles where no cellular service is available and act as routers to deliver information to destination nodes available within cellular coverage. In these cases, the design and deployment of such systems rely on proper modeling and characterization of signal propagation between the in-vehicle-to-in-vehicle communication of IoT devices. This study proposes models that can be used for such design and in similar environments with the end goal of improving the quality of service of these systems

and get them closer to the vision of self-management. The proposed models are compared with theoretical models that deviate from 6 to 23%.

## 2.2. Introduction

High modulation schemes require a high Signal to Noise ratio (S/N). This is because, for a given power level, the bit energy decreases if the data rate increases. It is also well known that for a given power the available data rate decreases with the increase of distance between the base station and mobile device.

While an overestimation of path loss can result in extensive coverage overlaps, an underestimation can lead to coverage holes. Path loss is a function of various factors such as free space losses, diffraction, reflection, transmission frequency, terrain, and many others. Numerous propagation models have been derived and studied, however; there is no single model can be applied for all the environments. As a result, the Quality of Service (QoS) of the whole cellular network depends on the selection of most suitable of the radio propagation model.

Models that are used for predicting the path loss in macro-cells, which are usually encountered in cellular networks, are called macroscopic propagation models. There are many of them and they have different levels of accuracy and complexity. In general, there is a tradeoff between model simplicity and its accuracy. Macroscopic



propagation models can be classified into three main categories: basic propagation models, statistical propagation models, and deterministic models. The free space model and the two-ray model are Basic propagation models are used to predict the path loss in a very simple way. The major assumption in free space propagation is that there is a clear line of sight (LOS) between transmitter and receiver, meaning that no obstructions exist.

Unlike the free space propagation model where there is only a direct path between the transmitter and the receiver, in the two-ray model, the received signal is a sum of two components results from two different paths. One of the drawbacks of the two-ray model is that it underestimates the path loss because of two major reasons. In practice, the loss is almost always frequency dependent. Second, in this model, the ground was assumed flat and smooth which is, in reality, not the case. The roughness of the terrain can lead to scattering which in turn affects the total value of the signal power and consequently the path loss [15].

The advent of IoT where every day “things” are connected together through the internet is expected to impact society and improve quality of life. There are two types of communication for IoT devices, one is the mesh network that each IoT device or sensor connects directly to another without the existence of cellular network (no coverage) and the second type of IoT communication is the cellular communication and in this type of communication there is no direct communication between an IOT

device and another but they communicate through a cellular network. One of the applications of IoT is the vehicle fleet management systems [15], [16]. This system can offer many services like improve customer service, increase productivity, reduce fuel cost and provide improved routing information. In the vehicle fleet management systems, vehicles can communicate with one another and to a control center. IoT devices are used to track the location of vehicles, prevent theft or accidents, monitor vehicle activity, and report management data to a vehicle's dashboard and wirelessly to a control center. Existing transmission links between existing taxi cab drivers and management office relies on the public mobile access radio (PMAR) to disseminate information; however, this mode of communication only supports voice data. Current vehicle systems, which are loaded with sensing devices, require support for data transmission (in addition to voice) between vehicles and to the control centers. XBee S2 Pro IoT nodes and other IoT devices can be used to establish a device-to-device mesh communication network on the vehicles where there is no cellular coverage at a point in time. The device in a vehicle can act as a router to another vehicle and has a Gateway-Digi XBee Cellular LTE Cat1 device to communicate to the cellular tower. This study aims to model the device-in-vehicle-to-device-in-vehicle communication path loss model using XBee ZigBee/IEEE 802.15.4 device that operates at 2.4GHz band. Accurate models for vehicle-to-vehicle (V2V) communication will ensure accurate information and data in the vehicle fleet

management system. Empirical path loss models are derived from measurements and they are compared with theoretical models such as the two-ray and free space models in literature [17]. These models can be used for link design in V2V networks.

The approach presented in this paper can also be used to characterize channel modeling for IoT cellular devices to perform device-to-device vehicle communication when they are available to the public. The manufacturer in [18] will soon release to the market Digi XBee Cellular LTE CatM1 that is designed for IoT sensor applications and a device requiring lower throughput. This manufacturer will also release to the public another device, Digi XBee Cellular LTE Cat NB1, also known as Narrowband-IoT that will support lower bandwidth, solves the problem of poor signal strength and range limitations, and perform device to device communication. The approach described in this study can be used to model the communication path loss when these devices become available.

### 2.3. Literature Review

Few studies have been made on propagation modeling for V2V communication, however, the measurement scenarios do not take into account intricacies of the communication environment, which differs from what is presented in this research. The authors in [19] present analytically derived V2V success probability near an

urban intersection for V2V communications. They simulate V2V with 5.9 GHz frequency and transmitting (Tx) power of 20 dBm to evaluate the probability of success or reliability for various scenarios of TX and receiving (RX) positions. They confirm that the analytically derived success model can be amended to fit various path loss models. Similarly, the authors in [20] propose a slope path loss model for V2V communication and check the accuracy of the model with actual measurements in the on-slope area of the road with the Berkeley Varitronics System. The system has TX power of 33 dBm TX power, and operating at 5.12 GHz band, the antenna connected to TX and RX is mounted at 0.9 m height on a cart. The authors confirm that the measured data agree fairly well with that computed proposed theoretical model. Also, propagation measurement for V2V communication within vehicle engine compartments is reported in [21], [22]. The authors in [23] provide measurement and analytical results for V2V propagation path loss and root-mean-square delay spread along the roadway. The authors determine the Doppler shift effect in a simulation scenario with a vehicle-to-infrastructure (V2I) path loss model and various V2V channel models [23].

After a thorough review of the literature, it is found that car-device-to-car-device communication modeling is not widely available or properly studied. The measurement scenarios described in the literature do not take into account devices inside a car or embedded in a car that communicates with another device embedded

in another car. Also, they do not report the state of vehicles (e.g., in motion or not) during experiments.

## 2.4. Methodology

### 2.4.1. Experimental Campaign and Measured Values

In the experimental set up used in this study, measurements are obtained using the method discussed in [24, 25, 26] with the aid of 3 dBm XBee S2ZB IoT nodes with a receiver sensitivity of -92 dBm and 18 dBm XBee Pro S2ZB IoT nodes with a receiver sensitivity of -102 dBm [27]. The nodes have linearly polarized omnidirectional antennas of 2.6 cm high and a gain of 1.5 dB. The nodes are portable devices with a dimension of approximately 3 x 3 x 2.6 cm. Direct sequence spread spectrum (DSSS) is a modulation technique used to shield against noise and interference [27]. The devices operate at a frequency band of 2.4 GHz with 250 kbps data and ZigBee/IEEE 802.15.4 protocol is used in the device implementation. A device is configured as a sink node and the other is configured as a router that route packets to the sink node every second. One device is connected to the laptop to serve as a means of collecting the measurements and the other node is powered by a 3.3v, 3000 mAH Lithium battery.

The 2 dBm XBee IoT nodes are attached to the inside floor of sedan and SUV car and at a point close to seat height in vertical polarization, with two people present in one car and the car remains in a spot in an urban environment. Another IoT device is placed in another sedan car with one person inside the car and the car is placed at an interval of 2.74 m from the static car. At each interval, path loss measurements and packet drop rates are obtained. The experiment is repeated with 18 dBm XBee IoT nodes with a 5 m distance interval between the vehicles. This means the distance between the TX node and RX node is approximately 6.52 m for up to 8 points as seen in Fig. 2.1. The measured path loss values are given in Tables 2.1 to 2.3.

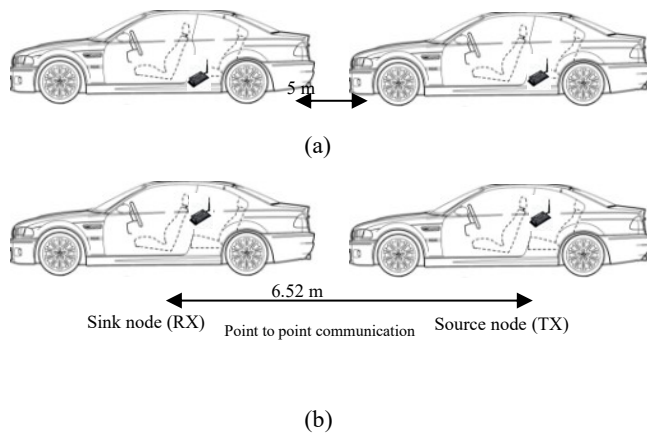


Fig. 2.1. Pictorial diagram for in-car measurement, (a) for a node on the car floor, (b) for a node at seat height.

TABLE 2.1  
AVERAGE PATH LOSS AT 2.74 m INTERVAL USING 3 dBm NODE

Node deployed in tree vegetation environment	Path loss (dB)							
	2.74 m	5.48 m	8.22 m	10.96 m	13.70 m	16.44 m	19.18 m	21.92 m
Sedan-to-Sedan, node on the car floor	60.88	65.00	74.00	-	-	-	-	-
Sedan-to-Sedan, node at seat height – T1	62.00	71.11	72.30	78.88	77.60	-	-	-
Sedan-to-SUV, node on the car floor	66.36	73.00	-	-	-	-	-	-
Sedan-to-Sedan, node at seat height – T2	60.00	63.40	67.30	69.00	72.84	75.00	83.22	87.10

TABLE 2.2  
AVERAGE PATH LOSS AT 6.52 m INTERVAL USING 18 dBm NODE

Node deployed in tree vegetation environment	Path loss (dB)							
	6.52 m	13.04 m	19.56 m	26.08 m	32.60 m	39.12 m	45.64 m	52.16 m
Sedan-to-Sedan, node on the car floor – T3	73.17	81.50	86.67	92.50	84.67	87.40	96.00	94.71
Sedan-to-Sedan, node at seat height – T4	62.25	71.00	74.40	75.50	79.50	79.00	83.20	-

TABLE 2.3  
SUMMARY OF PROPOSED MODELS, PARAMETERS AND PERCENTAGE  
DEVIATION

Environment	Proposed path loss models	Far-field path loss $P_f(d_o)$ (dB)	Path loss exponents ( $\alpha$ )	Shadowing values – $\sigma_{(dB)}$	R <sup>2</sup>	Deviation	Two-ray	FSPL
T1	$52.36 + 23.45 \log_{10} d$	52.36	2.3	9.6	0.94	<i>value</i>	6 % Close Predict	21 % Under Predict
T2	$43.79 + 28.07 \log_{10} d$	43.79	2.8	12.0	0.84	<i>value</i>	2 % Same Predict	17 % Under Predict
T3	$56.45 + 22.03 \log_{10} d$	56.45	2.2	8.0	0.80	<i>value</i>	9 % Close Predict	23 % Under Predict
T4	$44.41 + 22.76 \log_{10} d$	44.41	2.3	7.4	0.97	<i>value</i>	6 % Close Predict	11 % Under Predict



## 2.5. Preliminary Results and discussion

### 2.5.1. Empirical models

The path loss linear regression model was created using the values in the Tables 2.1 and 2.2 and the approach in [24] is shown in Figs. 2.2 to 2.5 Log-distance path loss model,  $PL(d)$  can be expressed as [17], [24]:

$$PL(d)_{[dB]} = PL(d_0)_{[dB]} + 10\gamma \log_{10} \left( \frac{d}{d_0} \right) + X_\sigma \quad (1)$$

where  $d_0$  is far-field distance or reference distance, typically chosen as 1m,  $d$  is the distance between transmitting node and receiving node (in meters),  $PL(d_0)_{[dB]}$  is the median path loss at reference distance, that is, the intercept, slope =  $10\gamma$ , where  $\gamma$  is the path loss exponent and  $X_\sigma$  is lognormal shadowing. Lognormal shadowing is the Gaussian random variable with zero mean and variance  $\sigma^2$ .

Similarly, some statistics used in this study for model significance test, that is, *MAPE* (Mean Absolute Percentage Error) and *Ts*, are provided in (2) and (3) respectively. *MAPE* expresses accuracy as a percentage of error [28]. *Ts* is used to check for bias in the models. A large *Ts* indicates a bias in the models.

$$MAPE = \frac{1}{n_j} \sum_{k=1}^{n_j} \left| \frac{eM_k - tM_k}{eM_k} \right| \times 100\% \quad (2)$$

$$Ts = \frac{\sum_{k=1}^{n_j} eM_k - tM_k}{(\sum_{k=1}^{n_j} |eM_k - tM_k|)/n_j} \quad (3)$$

where  $eM_k$  is the  $k^{th}$  empirical model value,  $tM_k$  is  $k^{th}$  theoretical model value,  $Ts$  is the tracking signal,  $MAPE$  is the mean absolute percentage error and  $n_j$  is the number of samples.

For accuracy of the model,  $Ts$  should be between -6, and 6 and  $MAPE$  should be less than 10 [28], [29]. Also, the statistics in (4) are used to test the significance of the proposed models.

$$MSE = \sum_{k=1}^{n_j} \frac{(eM_k - tM_k)^2}{n_j - 1}, RMSE = \sqrt{MSE} \quad (4)$$

where  $MSE$  is the means squared error and  $RMSE$  is the root mean squared error.

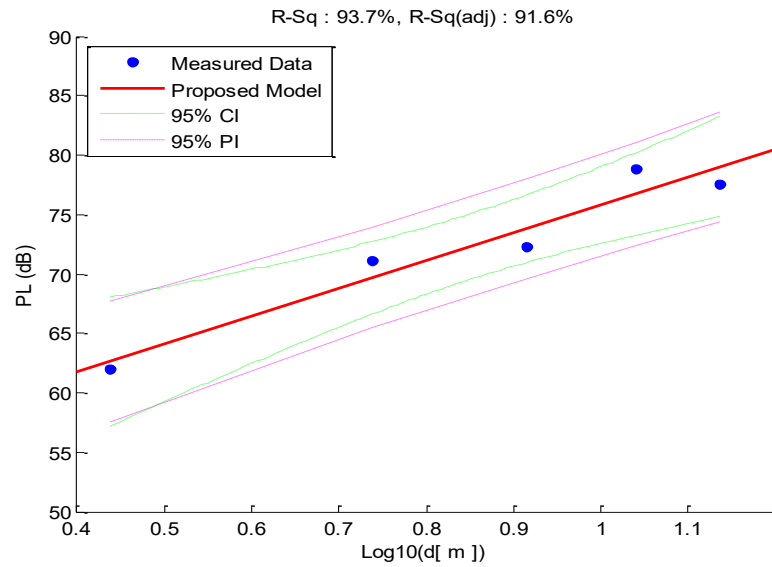


Fig. 2.2. Path loss model plot for Sedan-to-Sedan, a node on the car floor.

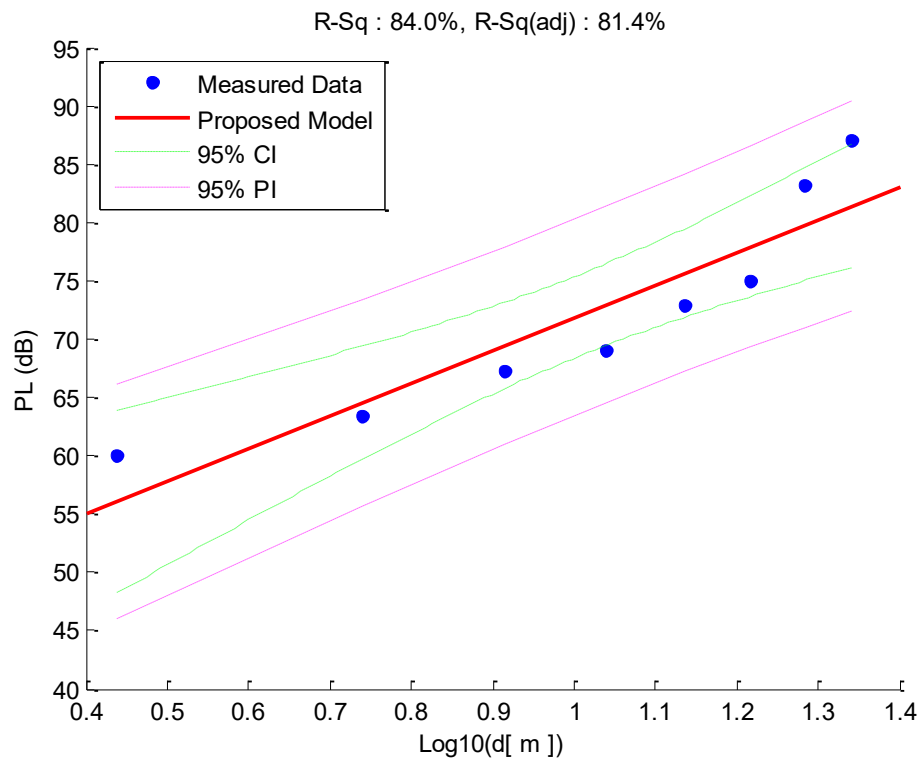


Fig. 2.3. Path loss model plot for Sedan-to-Sedan, a node at seat height.

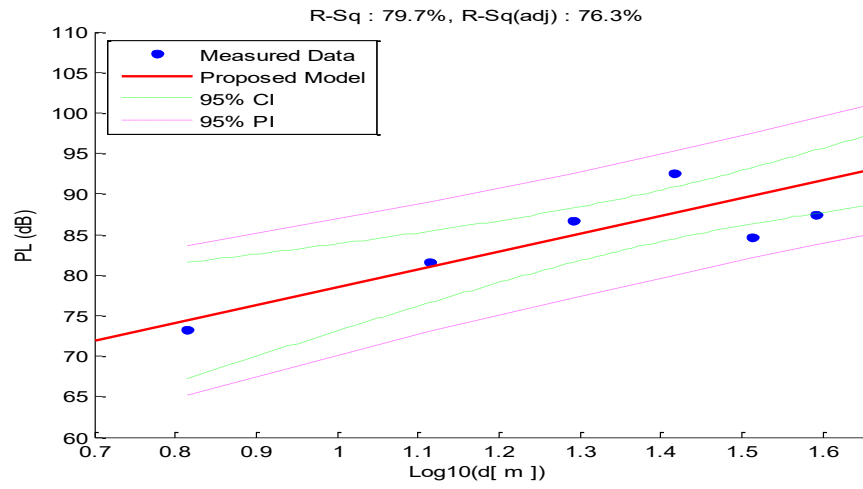


Fig. 2.4. Path loss model plot for Sedan-to-Sedan, a node on the car floor with 18 dBm node.

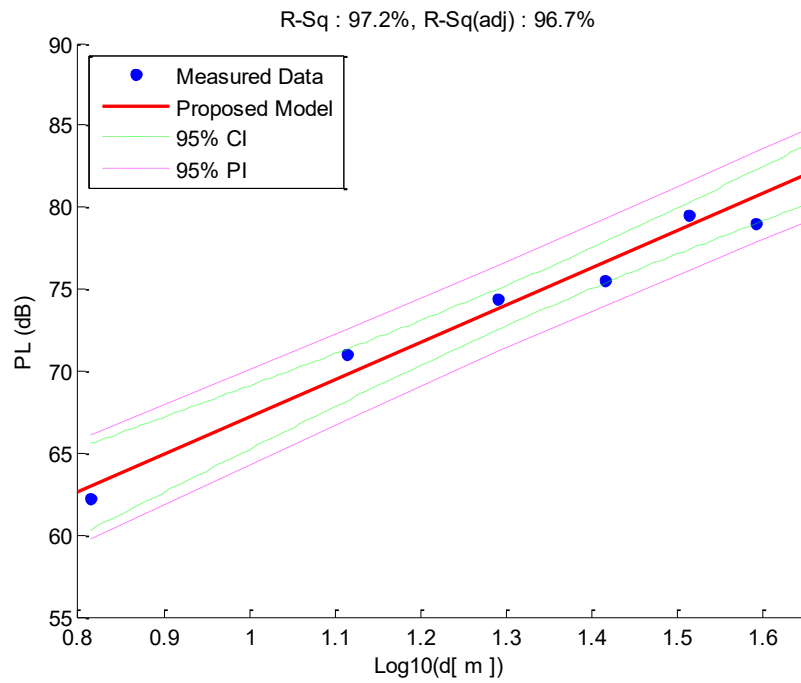


Fig. 2.5. Path loss model plot for Sedan-to-Sedan, a node at seat height with 18 dBm node.

TABLE 2.4  
STATISTICS FOR COMPARISON BETWEEN THEORETICAL MODELS AND  
PROPOSED T1 MODEL

<b>Models</b>	<b>MAPE (%)</b>	<b>MSE</b>	<b>RMSE</b>	<b>Ts</b>
<i>FSPL</i>	21	258	16	30
<i>two-ray</i>	6	64	8	28

The measured path loss values when 2 dBm is placed on the car floor is high at distance greater 5.48 m and connectivity is lost at 8.22 m. The signal blockage from the in-vehicle environment is too high for the low power node. When nodes are placed at seat height, the signal blockage is minimal. The path loss is also low when a high power node is used in the measurement. From the comparisons in Tables III and IV, it can be seen that the two-ray model results in a similar propagation model like the one proposed for V2V communication in this study. However, it can be seen that the free space model will under-predict when compared to the propagation model proposed in this research.

## Chapter 3

# Reliability Analysis of V2V Communications Link

### 3.1. Abstract

Reliable communication of information from vehicle-to-vehicle (V2V), vehicle-to/from-infrastructure (V2I) or vehicle-to/from-environments is critical in the implementation of the advent of autonomous vehicles and self-driving cars. Various units and subsystems of the ecosystem in which tiny IoT devices and sensor nodes are part, (are needed to be impeccable) deployed on the vehicles and in the environments to sense the environments and send information to a unit for processing and make decision per nanosecond of time. However, the heterogeneous environments and overall ecosystems pose reliability changes on the information transmitted to be processed by the ecosystem in order to guarantee the safety and functional operation of the ecosystem. This study examines the reliability of the communication model that can support the operation of self-driving cars ecosystem. It also shows semi-empirical energy per bit to noise spectral density, empirical radio propagation models and parameters for driving and transportation environment. These values and models are obtained from a combination of the experimental approach and analytical approach of additive white Gaussian noise

channel. They are used to ensure a reliable communication of wireless sensor nodes deployed in the environments for V2V and V2I. Also, the values and models are validated in theoretical and semi-analytical simulation scenarios. The result shows that both techniques are nearly identical. The semi-empirical approach, the proposed models, and values can be used for efficient planning and future deployments of autonomous vehicles and self-driving cars.

### 3.2. Introduction

There is a need to have accurate channel models able to predict the peculiarities of the vehicular propagation at ISM Band, especially as far as Vehicle-to-Vehicle (V2V) communications are concerned. Accurate radio channel models are crucial for the realistic evaluation of a vehicular communication system's performance. Some of the previous studies use free space and two ray models which are not suitable for Vehicle to Vehicle communication. Most of the previous studies that propose a path loss model using signal generator do not put into confirmation these significant factors (SINR, PDR, and BER) that determine the reliability of communication links. The results of models from signal generators can be used in real applications if the reliability of data and conspicuousness of nodes is not important and if the models from the portable actual nodes are not available. This study shows semi-empirical energy per bit to noise spectral density and parameters for a vehicle to vehicle

communications. These values and models are obtained from a combination of the experimental approach and analytical approach of additive white Gaussian noise channel. They are used to ensure a reliable communication of wireless sensor nodes in V2V communication.

### 3.3. Literature Review

V2V Channel modeling information is not widely studied. The previous study uses theoretical models such as free space and two ray models to design a communication link for V2V communication. The metrics that determine the quality or reliability of a communication link are received signal strength indication (RSSI), signal-to-interference-plus-noise ratio (SINR), packet-delivery ratio (PDR), and bit-error-rate (BER) [30]. These link quality indicators are not considered in the empirical path loss models provided in the literature and the implementation of the link budget.

The authors in [31] use the average Packet Reception Ratio (PRR), which measures the percentage of vehicles experiencing successful packet reception. They consider the successful reception is achieved if the Signal to Noise Ratio (SNR) experienced between the transmitting and receiving vehicles is above a predefined threshold, taken to be 0 dB in their simulations.

in [32], the authors study the channel modeling by two methods, the first is by calculating the impulse response of the channel depending on the positions of the



scatterers, the transmitter, and the receiver. The second method is by calculating the path loss of the channel for different environments depending on the distance between the receiver and the transmitter.

Furthermore, the work in [33] shows that only RSSI value is not a good indicator for describing the link reliability when external interference like multipath fading appears, which is more common for the wireless environment. Also measuring the RSSI for a fraction of frame and not measuring the distribution of SINR for the whole frame period is not determine the link reliability. Similarity, the authors in [34] reported on channel measurements for a parking garage, in the 5 GHz band. Results for propagation path loss and root-mean-square delay spread (RMS-DS) for Tx and Rx on the same floor, and on different floors for assessing communication system performance. In a related development, in [35] The authors propose a line-of-sight (LOS) path loss model in vehicle-to-vehicle (V2V) scenarios and provide a deep analysis of shadow fading in urban non-LOS (NLOS) scenarios by the deductive method with the proposed LOS model. commercial V2X platforms which are totally compliant with WAVE standards is used for calculating the strength of received signals to develop the V2V path loss model and compare it with the two large-scale fading models, two-ray ground reflection model, and long-distance path loss model. In [36] the authors made a study to analyze the coverage and capacity of LTE-M and NB-IOT in a rural area. The results show that LTE-M can provide

coverage for 9.9% of outdoor and indoor devices if the latter is experiencing 10 dB additional loss. However, for deep indoor users, NB-IoT is required and provides coverage for about 95% of the users. The NB-IoT can provide coverage for more than 95% of the devices due to its Maximum Coupling Loss being 164 dB as compared to LTE-M's 156 dB, so there is 8 dB additional MCL for NB-IoT over LTE-M. In the same vein, the authors in [37] propose a resource size control method to enhance the link reliability performance. The proposed method adopts the resource size (i.e., the number of RBs for a single message) according to the macroscopic vehicular parameters (e.g., vehicle density, number of lanes, message size, and communication range). In addition, they demonstrate the feasibility of applying the proposed method in a practical LTE-V2V setting. They present the required signaling procedure and the additional system overhead imposed by the proposed method. Likewise, in [38], the authors presented a model of the transmission characteristics of the propagation channel for hostile underground, underwater, and oil environments and he mentioned that the BER of a communication system depends mainly on three factors, the channel model, the SNR and the modulation technique used by the system. Also, the  $E_b/N_0$  is an important parameter in digital communication. It is the normalized signal-to-noise ratio (SNR) measure, also known as the "SNR per bit". It is especially useful when comparing the BER performance of different digital modulation schemes without taking bandwidth into

account. After thorough review of the literature, it is found that V2V communication performance using path loss indicators is not widely available or properly studied. The measurement scenarios described in the literature do not take into account devices inside a car or embedded in a car that communicate with another device embedded in another car. Also, they do not report the state of vehicles (e.g., in motion or not) during experiments.

### 3.4. Experimental Campaign

In the experimental set up used in this study, measurements are obtained using the method discussed in [39] with the aid of 3 dBm XBee S2ZB IoT nodes with a receiver sensitivity of -92 dBm and 18 dBm XBee Pro S2ZB IoT nodes with a receiver sensitivity of -102 dBm [42]. The nodes have linearly polarized omnidirectional antennas of 2.6 cm high and a gain of 1.5 dB. The nodes are portable devices with a dimension of approximately 3 x 3 x 2.6 cm. Direct sequence spread spectrum (DSSS) is a modulation technique used to shield against noise and interference. The devices operate at a frequency band of 2.4 GHz with 250 kbps data and ZigBee/IEEE 802.15.4 protocol is used in the device implementation. A IoT device is configured as a sink node and the other is configured as a router that route packets to the sink node every second. One device is connected to the laptop to serve as a means of collecting the measurements and the other node is powered by a 3.3v,

3000 mAH Lithium battery. The 2 dBm XBee IoT nodes are attached to the inside floor of sedan and SUV car and at a point close to seat height in vertical polarization, with two people present in one car and the car remains in a spot in an urban environment. Another IoT device is placed in another sedan car with one person inside the car and the car is placed at an interval of 2.74 m from the static car. At each interval, path loss measurements and packet drop rates are obtained. The experiment is repeated with 18 dBm XBee IoT nodes with a 5 m distance interval between the vehicles. This means the distance between the TX node and RX node is approximately 6.52 m for up to 8 points. The measured path loss values are given in Tables 3.1 to 3.3. Also, the path loss linear regression model was created using the values in the Tables I and II and the approach in, as [39] [40],[41] are shown in Table 3.3.

TABLE 3.1  
AVERAGE PATH LOSS AT 2.74 m INTERVAL USING 3 dBm NODE

Node deployed in tree vegetation environment	Path loss (dB)							
	2.74 m	5.48 m	8.22 m	10.96 m	13.70 m	16.44 m	19.18 m	21.92 m
Sedan-to-Sedan, node on the car floor	60.88	65.00	74.00	-	-	-	-	-
Sedan-to-Sedan, node at seat height – T1	62.00	71.11	72.30	78.88	77.60	-	-	-
Sedan-to-SUV, node on the car floor	66.36	73.00	-	-	-	-	-	-
Sedan-to-Sedan, node at seat height – T2	60.00	63.40	67.30	69.00	72.84	75.00	83.22	87.10

TABLE 3.2  
AVERAGE PATH LOSS AT 6.52 m INTERVAL USING 18 dBm NODE

Node deployed in tree vegetation environment	Path loss (dB)							
	6.52 m	13.04 m	19.56 m	26.08 m	32.60 m	39.12 m	45.64 m	52.16 m
Sedan-to-Sedan, node on the car floor – T3	73.17	81.50	86.67	92.50	84.67	87.40	96.00	94.71
Sedan-to-Sedan, node at seat height – T4	62.25	71.00	74.40	75.50	79.50	79.00	83.20	-

TABLE 3.3

SUMMARY OF PROPOSED MODELS, PARAMETERS AND PERCENTAGE  
DEVIATION

Environment	Proposed path loss models	Far-field path loss $P_l(d_0)$ (dB)	Path loss exponents ( $\alpha$ )	Shadowing values – $\sigma_{(dB)}$	R <sup>2</sup>	Deviation	Two-ray	FSPL
T1	$52.36 + 23.45 \log_{10} d$	52.36	2.3	9.6	0.94	<i>value</i>	6 % Close Predict	21 % Under Predict
T2	$43.79 + 28.07 \log_{10} d$	43.79	2.8	12.0	0.84	<i>value</i>	2 % Same Predict	17 % Under Predict
T3	$56.45 + 22.03 \log_{10} d$	56.45	2.2	8.0	0.80	<i>value</i>	9 % Close Predict	23 % Under Predict
T4	$44.41 + 22.76 \log_{10} d$	44.41	2.3	7.4	0.97	<i>value</i>	6 % Close Predict	11 % Under Predict

### 3.5. Analysis and Results

The measured or empirical communication parameters and values are given in Table 3.3. In this study, IoT hardware used for WSN deployments includes the XBee sensor node which employs O-QPSK (Offset quadrature phase-shift keying) modulation schemes with a direct sequence spread spectrum (DSSS). The intended receiver of the DSSS signal can recover a weak signal as a result of channel noise and interference with the aid of processing and coding gain used on the device.

The transmitted signal has a low probability of being intercepted [40], [41]. Therefore, co-channel interference can be neglected for WSN and adjacent channel interference can be regarded as random and modeled into the noise power. Accordingly, the signal-to-noise and interference ratio (SNIR) is:

$$SNIR[dB] = 10 \log_{10} \left( \frac{P_r}{P_0 + \sum_{j=1}^m I_j} \right) \quad (1)$$

where  $P_r$  is the received signal strength,  $P_0$  is the noise power,  $I_j$  is the interference from node  $j$ , and  $m$  is the number of neighbors that contribute to the interference.

Equation 1 can be simplified for WSN as signal-to-noise ratio (SNR) per distance as:

$$SNR(d)_{[dB]} = P_t - PL(d) - P_n \quad (2)$$

where  $P_t$  is the transmit power (in  $dBm$ ),  $PL(d)$  is the multi-path path loss in ( $dB$ ),  $P_n$  is the noise floor in ( $dBm$ ).

Similarly,  $PL(d)$  can be expressed as:

$$PL(d)_{[dB]} = PL(d_0)_{[dB]} + 10\gamma \log_{10} \left( \frac{d}{d_0} \right) + X_\sigma \quad (3)$$

where  $d_0$  is far-field distance or reference distance, typically chosen as 1m,  $d$  is the

distance between transmitting node and receiving node (in meters),  $PL(d_0)_{(dB)}$  is the median path loss at reference distance, that is, the intercept, slope =  $10\gamma$ , where  $\gamma$  is the path loss exponent and  $X_\sigma$  is lognormal shadowing. Lognormal shadowing is the Gaussian random variable with zero mean and variance  $\sigma^2$ .

Also,

$$P_n \text{ [dBm]} = 10\log_{10}(KTB_n) + F_{dB} \quad (4)$$

where  $F_{dB}$  is the noise figure,  $B_n$  is the noise bandwidth in (Hz),  $KT = 4.1 \times 10^{-18} \text{ mW/Hz}$ , with Boltzmann's constant,  $K$  at room temperature,  $T$ .

If (3) and (4) are substituted into (2), it becomes:

$$SNR(d)_{[dB]} = P_t - PL(d_0)_{[dB]} - 10\gamma \log_{10}\left(\frac{d}{d_0}\right) - X_\sigma - 10\log_{10}(KTB_n) - F_{dB} \quad (5)$$

It can be shown from (5) that signal-to-noise ratio  $SNR(d)_{[dB]}$  depends on the environment type (characterized by  $PL(d_0)_{[dB]}$ ,  $\gamma$ ), the distance, the transmit power, the multi-path shadowing effect ( $X_\sigma$ ), and the noise bandwidth. As the distance increases, the  $SNR(d)_{[dB]}$  decrease.

Similarly, energy per bit to noise spectral density,  $\frac{E_b}{N_{0linear}}$  is related to signal-to-noise ratio in linear as:



$$\frac{E_b}{N_{0linear}} = SNR_{linear} \cdot \frac{B}{R_b} \quad (6)$$

where  $R_b$  is the data rate (in bits/s),  $B$  is the bandwidth per channel in (Hz),

$$SNR_{linear} = 10^{0.1 \times SNR(d)_{[dB]}}$$

Also, the probability of error or bit error rate (BER) for O-QPSK according to Shannon theorem is:

$$BER = Q\left(\sqrt{2 \frac{E_b}{N_{0linear}}}\right) \quad (7)$$

Finally, the spectral efficiency ( $SPE$ ) in b/s/Hz is:

$$SPE = \log_{10}(1 + SNR_{linear}) \quad (8)$$

Therefore, using the measured path loss indicators, this study obtains the V2V communications performance parameters. From the experiments, the values for the following parameters-  $PL(d_0)_{[dB]}$ ,  $\gamma$ , and  $X_\sigma$  are obtained which are in turn used in (5) to establish semi-empirical models for  $\frac{E_b}{N_{0(dB)}}$  and  $SNR_{(dB)}$ .

Therefore, (5) and (6) now become:

$$\begin{aligned} SNR(d)_{[dB]_{s_e}} &= P_{t(v)} - PL(d_0)_{[dB]_{s_e}} - 10\gamma_{s_e} \log_{10}\left(\frac{d_{s_e}}{d_{0(s_e)}}\right) - X_{\sigma(s_e)} \\ &\quad - 10\log_{10}(KTB_{n(v)}) \end{aligned} \quad (9)$$

$$\frac{E_b}{N_{0(dB)s_e}} = SNR(d)_{[dB]s_e linear} \cdot \frac{B_{(v)}}{R_{b(v)}} \quad (10)$$

where  $SNR(d)_{[dB]s_e}$  is the semi-empirical signal-to-noise ratio,  $\frac{E_b}{N_{0(dB)s_e}}$  is semi-empirical energy per bit to noise spectral density,  $P_{t(v)}$  is the manufacturer specified transmit power (18 dBm) for XBee Pro S2ZB sensor node,  $d_{0(s_e)}$  is the experimentally chosen far-field distance,  $d_{s_e}$  is the experimentally chosen distances between transmitting nodes and receiving nodes (in meters),  $PL(d_0)_{[dB]s_e}$  is the experimentally obtained median path loss at reference distance,  $\gamma_{s_e}$  is the experimentally obtained path loss exponent,  $B_{n(v)}$  is manufacturer specified bandwidth (2.4GHz),  $X_{\sigma(s_e)}$  is experimentally obtained lognormal shadowing,  $R_{b(v)}$  is the manufacturer specified data rate (250000 bits/s) for the device, and  $B_{(v)}$  is the manufacturer specified bandwidth per channel (100 MHz or 150 MHz).

The measured or empirical communication parameters and values are given in Tables 3.1,3.2,3.3. These parameters are substituted into (9) and (10) to obtain  $SNR(d)_{[dB]s_e}$  and  $\frac{E_b}{N_{0(dB)s_e}}$  respectively. Using the obtained values of  $SNR(d)_{[dB]s_e}$  and  $\frac{E_b}{N_{0(dB)s_e}}$ , the bit error rate and spectral efficiency are also calculated. It is observed that as the distance increases, the SNR decreases as shown

in Fig. 3.1. The calculated spectral efficiency is plotted against the calculated energy per bit to noise spectral density as shown in Figs. 3.2 and 3.3. In the region below the curve in Fig. 3.3, that is, the region where the  $\frac{E_b}{N_0(dB)_{S_e}}$  is greater than  $-1.59$ , with blue line in Fig. 3.3, reliable communication is possible, and in the region above the curve, that is where  $\frac{E_b}{N_0(dB)_{S_e}}$  is less than  $-1.59$ , reliable communication is not guaranteed [41].

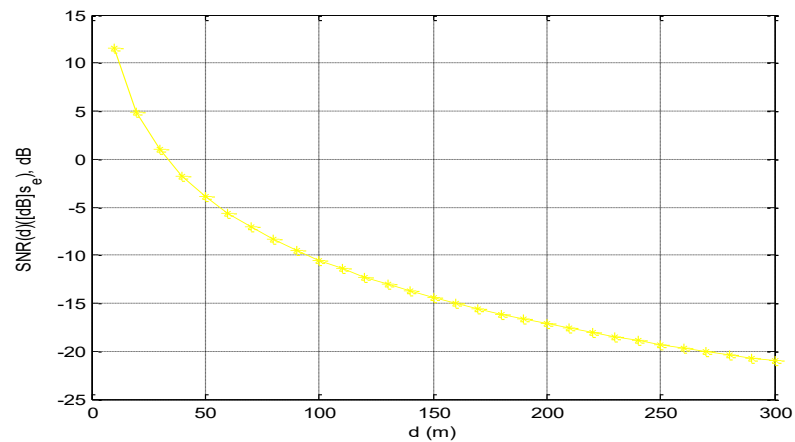


Fig. 3.1. Plot for SNR against distance.

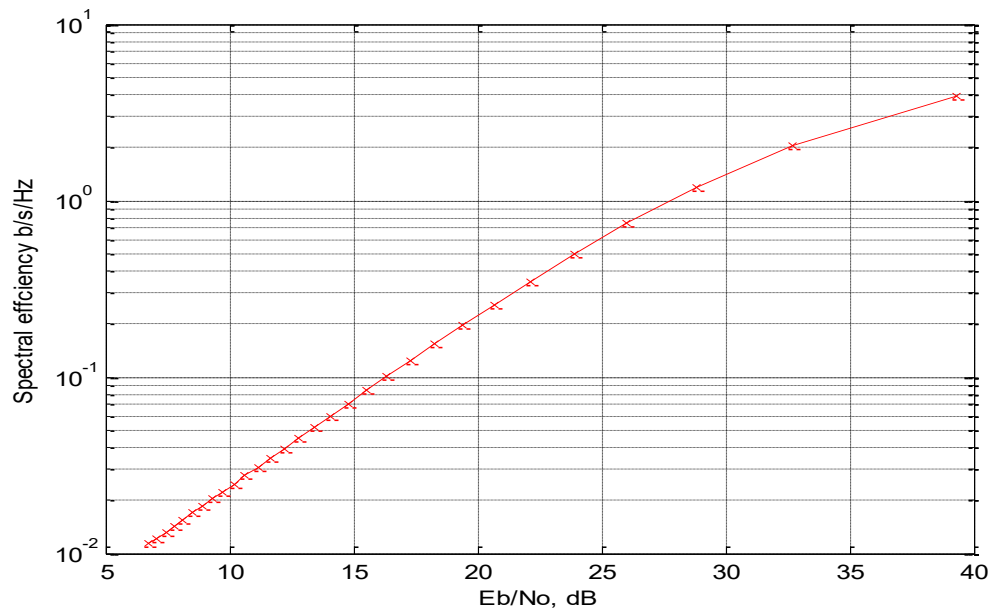


Fig.3.2. Spectral efficiency vs energy per bit to noise spectral with higher values of

$$\frac{E_b}{N_0(dB)}$$

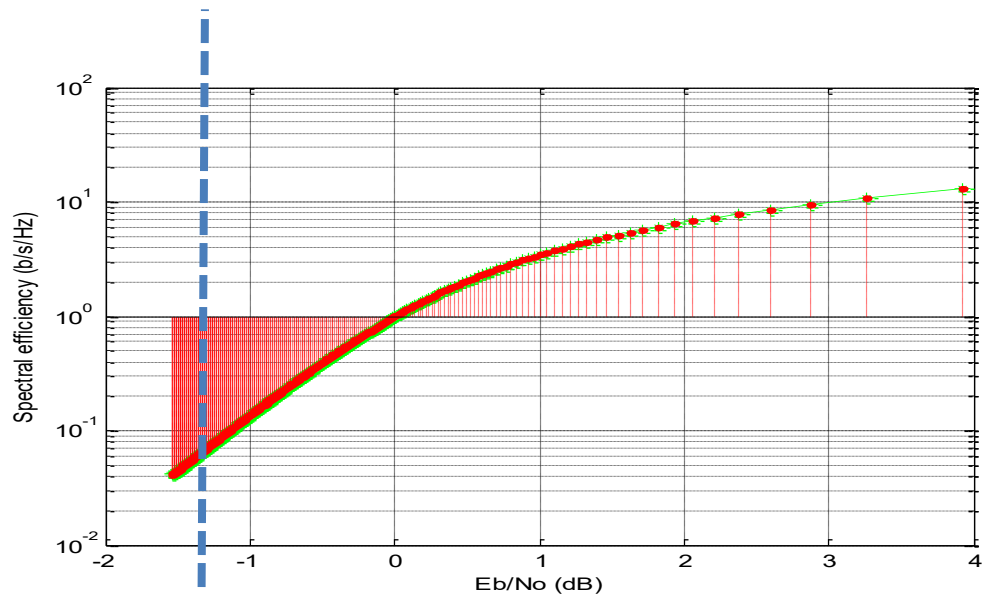


Fig. 3.3. Plot for Spectral efficiency vs energy per bit to noise spectral for V2V communications

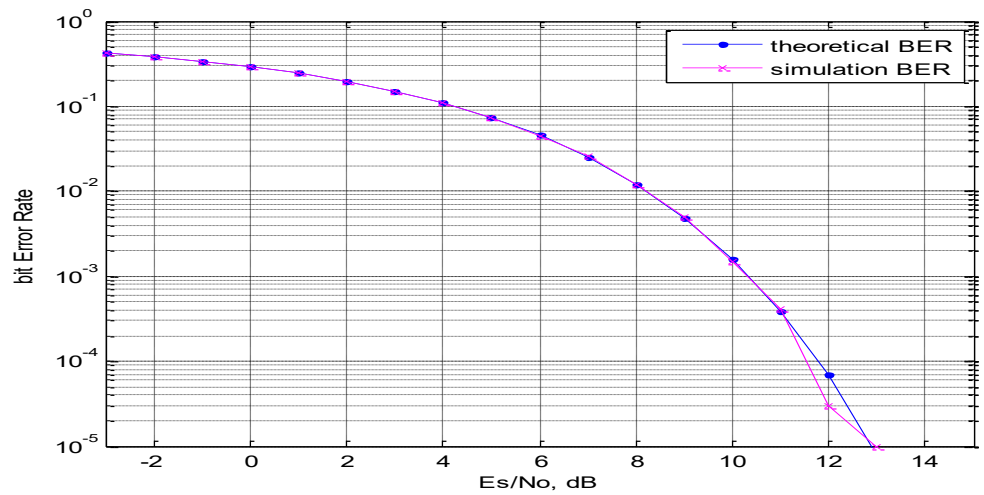


Fig.3.4. The plot of theoretical and simulated BER vs energy per bit to noise spectral

Similarly, the calculated energy per bit to noise spectral density,  $\frac{E_b}{N_0(dB)_{s_e}}$  is used in theoretical and semi-analytical simulation as shown in Fig.3.4. The result shows that the error rates obtained using the two techniques are nearly identical. The noticeable discrepancies are due to the phase offset in the channel model. According to [41],[42],  $\frac{E_b}{N_0(dB)_{s_e}}$  must be greater than  $-1.59$  to have reliable communication. It can be observed that  $\frac{E_b}{N_0(dB)_{s_e}} = -1.5855$  at distance less than 1130 m between two nodes for the V2V communication link with static cars.

Therefore, if the measured parameters ( $PL(d_0)_{[dB]}$ ,  $\gamma$ ,  $X_\sigma$ ) are not accurate as a result of an inaccurate model or not considered in modeling, it will, in turn, produce a bad signal-to-noise ratio. Hence, it will make the communication link unreliable which could be disastrous especially in the deployment of LPWAN for V2V. As conclusion, this study experimentally reports the energy per bit to noise spectral density that describes communication performance at a particular distance in fleet vehicular environments. This study presents empirical path loss models for V2V communication in vehicle fleet management system. Measurements are obtained for V2V communication with Sedan and SUV cars in urban environment in static positions. The empirical models and parameters can be used for planning and deployment of V2V devices in similar scenarios. Alternatively, network designers for V2V can also use two-ray model with similar results.

## References

- [1] 4G Americas, “Understanding 3GPP Release 12 Standards for HSPA+ and LTE-Advanced Enhancements,” 3GPP Release 12 Executive Summary, <http://www.5gamericas.org/understanding-3gpp-release-12-standards-for-hspa-and-lte-enhancements>, February 2015.
- [2] 3GPP, “Standardization of Machine-Type Communications V0.2.4,” June 2016.
- [3] D. W. Matolak, “Modeling the vehicle-to-vehicle propagation channel: A review,” *Radio Sci.*, vol. 49, no. 9, pp. 721–736, 2014.
- [4] M. Hamid and I. Kostanic, “Path Loss Models for LTE and LTE-A Relay Stations,” *Univers. J. Commun. Netw.*, vol. 1, no. 4, pp. 119–126, 2013.
- [5] F. Text, “LPWANs set to take on cellular for IoT applications says Beecham Research report ; LPWANs to provide 26 % of the total IoT connectivity market with over 345 million connections by 2020,” pp. 1–2, 2016.
- [6] R. Ratasuk, N. Mangalvedhe, and A. Ghosh, “Overview of LTE Enhancements for Cellular IoT,” pp. 2293–2297, 2015.
- [7] Huawei, “Narrow Band IoT & M2M - NB-IoT: Enabling New Opportunities,” White Paper, <https://gsacom.com/paper/nb-iot-enabling-new-opportunities>, 2016.

- [8] J. Gozalvez and S. Mobile, “New 3GPP Standard for IoT,” no. March, pp. 14–20, 2016.
- [9] Qualcomm Incorporated, “Narrow Band IoT (NB-IOT),” 3GPP TSG Meeting # 69, September 14-16,2015.
- [10] Ray, B. “What is LTE-M?,” Link Labs, <https://www.link-labs.com/blog/what-is-lte-m>, January 27, 2017.
- [11] Ray, B., “Three 3GPP IoT Technologies to Get Familiar with.” Link Labs, [https://www.link-labs.com/blog/lte-iot-technologies?utm\\_campaign=New%20Work%20Flow&utm\\_source=hs\\_automation&utm\\_medium=email&utm\\_content=35465814&\\_hsenc=p2ANqtz\\_kfepe9fc\\_1qlgxhgi32wdldgah3j7mxvpbh2bcfufyyvdmpv9qrhtw5psp8ffaayyxgh1pur3ij47psftd-zpd311g&\\_hsmi](https://www.link-labs.com/blog/lte-iot-technologies?utm_campaign=New%20Work%20Flow&utm_source=hs_automation&utm_medium=email&utm_content=35465814&_hsenc=p2ANqtz_kfepe9fc_1qlgxhgi32wdldgah3j7mxvpbh2bcfufyyvdmpv9qrhtw5psp8ffaayyxgh1pur3ij47psftd-zpd311g&_hsmi), November 29, 2017.
- [12] AK Emarievbe, J. Koepp, and T. Opferman, “Emerging Communication Technologies Enabling the Internet of Things,” Rohde & Schwarz, September 2016.
- [13] Link Labs, “Symphony Link - Internet of Things Wireless LPWA,” <https://www.link-labs.com/symphony>, April 16, 2020.
- [14] M. D. Hamid, “Measurement-Based Statistical Model for Path Loss Prediction for Relaying Systems Operating in 1900 MHz Band,” no. December 2014.



- [15] J. Tan and S. G. Koo, "A Survey of Technologies in the Internet of Things," in *IEEE International Conference on Distributed Computing in Sensor Systems*, Marina Del Rey, CA, 2014.
- [16] A. W. Burange and H. D. Misalkar, "Review of Internet of Things in Development of Smart Cities with Data Management & Privacy," in *Computer Engineering and Applications (ICACEA), IEEE International Conference on Advances*, Ghaziabad, 2015.
- [17] J. S. Seybold, *Introduction to RF Propagation*, John Wiley and Sons Inc., 2005.
- [18] Digi Xbee, "The New DIGI XBEE Embedded cellular Modems," <https://www.digi.com/lp/xbee/hardware#protocols>, 2017.
- [19] M. Abdulla, E. Steinmetz and H. Wymeersch, "Vehicle-to-Vehicle Communications with Urban Intersection Path Loss Models," in *2016 IEEE Globecom Workshops (GC Wkshps)*, 2016.
- [20] P. Liu, D. W. Matolak, B. Ai and R. Sun, "Path Loss Modeling for Vehicle-to-Vehicle Communication on a Slope," *IEEE Transactions on Vehicular Technology*, vol. 63, no. 6, pp. 2954 - 2958, 2014.

- [21] H. Kamoda, S. Kitazawa, N. Kukutsu, K. Kobayashi and T. Kumagai, "Microwave Propagation Channel Modeling in a Vehicle Engine Compartment," *IEEE Transactions on Vehicular Technology*, vol. 65, no. 9, pp. 6831 - 6841, 2016.
- [22] U. Demir, U. C. Bas, and C. S. Ergen, "Engine Compartment UWB Channel Model for Intravehicular Wireless Sensor Networks," *IEEE Transactions on Vehicular Technology*, vol. 63, no. 6, pp. 2497 - 2505, 2014.
- [23] S.-K. Noh, P.-j. Kim and J.-H. Yoon, "Doppler effect on V2I path loss and V2V channel models," in *International Conference on Information and Communication Technology Convergence (ICTC)*, 2016.
- [24] T. O. Olasupo, C. E. Otero, O. K. Olasupo and I. Kostanic, "Empirical Path Loss Models for Wireless Sensor Network Deployments in Short and Tall Natural Grass Environments," *IEEE Transactions on Antennas & Propagation*, vol. 64, no. 9, pp. 4012-4021, 2016.
- [25] A. AlSayyari, I. Kostanic, and C. E. Otero, "An empirical path loss model for wireless sensor network deployment in an artificial turf environment," in *IEEE 11th International Conference on Networking, Sensing and Control (ICNSC)*, 2014.

- [26] A. AlSayyari, I. Kostanic, and C. E. Otero, "An empirical path loss model for wireless sensor network deployment in a concrete surface environment," in 2015 IEEE 16th Wireless and Microwave Technology Conference (WAMICON), 2015.
- [27] "ZigBee RF Modules documentation," 2015. [Online]. Available: <http://ftp1.digi.com/support/documentation/90000976.pdf>. [Accessed 3 July 2016].
- [28] B. Mahadevan, Operation Management: Theory and Practice, 1st ed., Prentice Hall, 2009, pp. 274-281.
- [29] C. Bozarth, "Measuring Forecast Accuracy: Approaches to Forecasting: A Tutorial," SCRC Articles Library, 25 January 2011.
- [30] K. O. Olasupo, I. Kostanic, C. E. Otero, and T. O. Olasupo, "Link performance modeling of wireless sensor network deployment for mission-critical applications (underground deployment)," 2017 16th Annu. Mediterr. Ad Hoc Netw. Work. Med-Hoc-Net 2017, 2017.
- [31] M. Giordani, T. Shimizu, A. Zanella, T. Higuchi, O. Altintas, and M. Zorzi, "Path loss models for V2V mmWave communication: Performance evaluation and open challenges," 2019 IEEE 2nd Connect. Autom. Veh. Symp. CAVS 2019 - Proc., 2019.

- [32] M. Kihl, K. Bür, F. Tufvesson, and J. L. A. Ojea, "Simulation modeling and analysis of a realistic radio channel model for V2V communications," 2010 Int. Congr. Ultra Mod. Telecommun. Control Syst. Work. ICUMT 2010, pp. 981–988, 2010.
- [33] S. Woo and H. Kim, "An empirical interference modeling for link reliability assessment in wireless networks," *IEEE/ACM Trans. Netw.*, vol. 21, no. 1, pp. 272–285, 2013.
- [34] R. Sun, D. W. Matolak, and P. Liu, "Parking garage channel characteristics at 5 GHz for V2V applications," *IEEE Veh. Technol. Conf.*, pp. 1–5, 2013.
- [35] J. Joo, O. S. Eyobu, D. S. Han, and H. J. Jeong, "Measurement-based V2V path loss analysis in urban NLOS scenarios," *Int. Conf. Ubiquitous Futur. Networks, ICUFN*, vol. 2016-August, pp. 73–75, 2016.
- [36] M. Lauridsen, "Coverage and Capacity Analysis of LTE-M and NB-IoT in a Rural Area," *Veh. Technol. Conf. 2016 Ieee 84th*, 2016.
- [37] Y. Park, T. Kim, and D. Hong, "Resource size control for reliability improvement in cellular-based V2V communication," *IEEE Trans. Veh. Technol.*, vol. 68, no. 1, pp. 379–392, 2019.
- [38] M. A. Akkaş, "Channel Modeling of Wireless Sensor Networks in Oil," *Wirel. Pers. Commun.*, vol. 95, no. 4, pp. 4337–4355, 2017.

- [39] I. Oraibi, C. E. Otero, and T. O. Olasupo, "Empirical path loss model for vehicle-to-vehicle IoT device communication in fleet management," in 2017 16th Annual Mediterranean Ad Hoc Networking Workshop, Med-Hoc-Net 2017, 2017.
- [40] I. F. Akyildiz, *Wireless Sensor Network*, Wiley, 2010.
- [41] G. J. Proakis and M. Salehi, *Communication Systems Engineering*, Pearson, 2001.
- [42] S. Verdú, "Spectral Efficiency in the Wideband Regime," *IEEE Transactions on Information Theory*, vol. 48, no. 6, pp. 1319 - 1343, 2002.